



This is a repository copy of *Identification of Coupled Map Lattice Models of Complex Spatio-Temporal Patterns*.

White Rose Research Online URL for this paper:
<http://eprints.whiterose.ac.uk/83988/>

Version: Published Version

Monograph:

Coca, D. and Billings, S.A. (2000) Identification of Coupled Map Lattice Models of Complex Spatio-Temporal Patterns. Research Report. ACSE Research Report 782 . Department of Automatic Control and Systems Engineering

Reuse

Unless indicated otherwise, fulltext items are protected by copyright with all rights reserved. The copyright exception in section 29 of the Copyright, Designs and Patents Act 1988 allows the making of a single copy solely for the purpose of non-commercial research or private study within the limits of fair dealing. The publisher or other rights-holder may allow further reproduction and re-use of this version - refer to the White Rose Research Online record for this item. Where records identify the publisher as the copyright holder, users can verify any specific terms of use on the publisher's website.

Takedown

If you consider content in White Rose Research Online to be in breach of UK law, please notify us by emailing eprints@whiterose.ac.uk including the URL of the record and the reason for the withdrawal request.



eprints@whiterose.ac.uk
<https://eprints.whiterose.ac.uk/>

IDENTIFICATION OF COUPLED MAP LATTICE MODELS OF
COMPLEX SPATIO-TEMPORAL PATTERNS

D. COCA



S.A. BILLINGS

Department of Automatic Control and Systems Engineering,
University of Sheffield
Sheffield, S1 3JD,
UK

Research Report No. 782
October 2000

Identification of Coupled Map Lattice Models of Complex Spatio-Temporal Patterns

D. COCA S.A. BILLINGS

Department of Automatic Control and Systems Engineering,
University of Sheffield,
Sheffield S1 3JD, UK

Abstract

A new method for the identification of nonlinear Coupled Map Lattice (CML) equations from measured spatio-temporal data is introduced. The application of the algorithm is demonstrated using chaotic two dimensional spatio-temporal patterns generated from interacting populations and the resulting models are validated by computing the attractors and the largest Lyapunov exponents.

1 Introduction

Complex spatio-temporal patterns can be observed in a variety of spatially extended systems in fields as diverse as chemistry, biology, engineering and ecology [14, 5, 3, 10]. In recent years, there has been a growing interest in the study of pattern formation phenomena driven in part by the large number of practical applications which would benefit from understanding and possibly controlling the formation of spatio-temporal patterns.

Normally the study of the formation and evolution of spatio-temporal patterns requires a model. In most cases such a model would be derived based on theoretical considerations, starting from the basic laws of physics or chemistry for example. Very often however finding the equations which describe the phenomena using an analytical modelling approach will fail to produce a good model because either the interactions involved are too complex (when the system is highly nonlinear for example) or when there are no established laws on which to base the choice of the model (as in most socio-economic phenomena for example).

The Coupled Map Lattice (CML) has been originally introduced as a spatial counterpart of lumped discrete dynamical systems and can be used to represent spatio-temporal phenomena which is discrete in time and space. CML can also provide approximate finite-dimensional models of infinite-dimensional systems which are normally represented in terms of Partial Differential Equations (PDE's) [15, 2, 4]. The study of CML's has revealed a wide range of spatio-temporal behaviours including spiral waves, spatio-temporal intermittency and chaos [7, 8, 6, 9, 12].

This paper proposes a new approach of identifying a CML model from data that describes the dynamics of the observed spatio-temporal system. The method is applied to identify alternative equations for a CML model proposed by Solé and Valls (1992) to describe the spatio-temporal dynamics of interacting (predator-prey) populations. For different choices of parameters this model exhibits various spatial patterns including spiral waves, chaotic and periodic dynamics. In the present study the CML model is identified in the chaotic domain and then validated by computing local phase plots and the largest Lyapunov exponents.



2 The CML Model

Consider the d -dimensional lattice \mathcal{I} consisting of the set of all integer coordinate vectors $i = (i_1, \dots, i_d) \in \mathbb{Z}^d$. A general CML model defined over \mathcal{I} can be written as

$$x_i(t) = f_l(\mathbf{q}^{-n_x} x_i(t), \mathbf{q}^{-n_u} u_i(t)) + f_c(\mathbf{q}^{-n_x} x_i(t), \mathbf{q}^{-n_u} u_i(t), \mathbf{s}^{m_x} \mathbf{q}^{-n_x} x_i(t), \mathbf{s}^{m_u} \mathbf{q}^{-n_u} u_i(t)) \quad (1)$$

where \mathbf{q}^{-n} is a (temporal) backward shift operator

$$\mathbf{q}^{-n} = (q^{-1}, q^{-2}, \dots, q^{-n}) \quad (2)$$

and \mathbf{s}^m is a multi-valued spatial shift (translation) operator

$$\mathbf{s}^{m_x} = (s^{p_x^1}, s^{-p_x^1}, \dots, s^{p_x^{m_x}}, s^{-p_x^{m_x}}) \quad (3)$$

$$\mathbf{s}^{m_u} = (s^{p_u^1}, s^{-p_u^1}, \dots, s^{p_u^{m_u}}, s^{-p_u^{m_u}}) \quad (4)$$

such that

$$\mathbf{q}^{-n_x} x_i(t) = (x_i(t-1), \dots, x_i(t-n_x)) \quad (5)$$

$$\mathbf{q}^{-n_u} u_i(t) = (u_i(t-1), \dots, u_i(t-n_u)) \quad (6)$$

and

$$\mathbf{s}^{m_x} x_i = (x_{i+p_x^1}, x_{i-p_x^1}, \dots, x_{i+p_x^{m_x}}, x_{i-p_x^{m_x}}) \quad (7)$$

$$\mathbf{s}^{m_u} u_i = (u_{i+p_u^1}, u_{i-p_u^1}, \dots, u_{i+p_u^{m_u}}, u_{i-p_u^{m_u}}) \quad (8)$$

where $p_x^j, p_u^j \in \mathbb{Z}^d$ are spatial translation multi-indexes.

In equation (1) $f : \mathcal{X}_i^{n_x+m_x} \times \mathcal{U}_i^{n_u+m_u} \rightarrow \mathcal{X}_i$ is a differentiable map depending on the local state and input variables at node i , $x_i \in \mathcal{X}_i$ and $u_i \in \mathcal{U}_i$ and on the variables at neighbouring sites. The function $f(\cdot)$ is assumed symmetric or anti-symmetric with respect to the coupling variables such that

$$f_c(\mathbf{q}^{-n_x} x_i(t), \mathbf{q}^{-n_u} u_i(t), x_{i+p_x^1}, x_{i-p_x^1}, \dots, x_{i+p_x^{m_x}}, x_{i-p_x^{m_x}}, u_{i+p_u^1}, u_{i-p_u^1}, \dots, u_{i+p_u^{m_u}}, u_{i-p_u^{m_u}}) = \quad (9)$$

$$\pm f_c(\mathbf{q}^{-n_x} x_i(t), \mathbf{q}^{-n_u} u_i(t), x_{i-p_x^1}, x_{i+p_x^1}, \dots, x_{i-p_x^{m_x}}, x_{i+p_x^{m_x}}, u_{i-p_u^1}, u_{i+p_u^1}, \dots, u_{i-p_u^{m_u}}, u_{i+p_u^{m_u}}) \quad (10)$$

Diffusion processes for example, are generally modelled using symmetric coupling functions while anti-symmetric coupling is associated with the modelling of open flows. Note that the CML described by equation (1) is very general and includes most common CML's described in the literature as special cases. In many examples for instance the coupling function $f_c(\cdot)$ depends only of the coupling variables. However, the inclusion of local variables (usually in a multiplicative manner) in the coupling function ensures that the CML can represent a wider range of nonlinear spatio-temporal phenomena.

Consider the CML model proposed by Solé and Valls (1992).

$$x_i(t) = \mu x_i(t-1)[1 - x_i(t-1)] \exp[-\beta y_i(t-1)] + D_1 \nabla^2 x_i(t-1) \quad (11)$$

$$y_i(t) = x_i(t-1)\{1 - \exp[-\beta y_i(t-1)]\} + D_2 \nabla^2 y_i(t-1) \quad (12)$$

Here $i = (i_1, i_2) \in \mathbb{Z}^2$ and

$$\begin{aligned} \nabla^2 x_{i_1, i_2}(t-1) &= x_{i_1-1, i_2}(t-1) + x_{i_1+1, i_2}(t-1) + x_{i_1, i_2-1}(t-1) \\ &+ x_{i_1, i_2+1}(t-1) - 4x_{i_1, i_2}(t-1) \end{aligned} \quad (13)$$

This corresponds to the following spatial translation operator

$$\mathbf{s}^2 = (s^{p^1}, s^{-p^1}, s^{p^2}, s^{-p^2}) \quad (14)$$

with $p^1 = (1, 0)$, $p^2 = (0, 1)$.

This model can exhibit various spatial patterns including spiral waves, chaotic and periodic dynamics. The data used for the identification was generated by simulating the CML model with $\mu = 4, \beta = 5$, $D_1 = 0.001$, $D_2 = 0.20$ for 6000 steps over a 256×256 lattice starting from randomly generated initial populations with 50 initial seeds [14] and periodic boundary conditions.

For this choice of simulation parameters the CML model is chaotic. Although in such a case no well-defined patterns are expected to appear, the model exhibits robust spiral waves which move through the lattice. The largest Lyapunov exponent, calculated using the global populations [14]

$$X(t) = \sum_{i \in \mathcal{I}} x_i(t) \quad (15)$$

was used to characterise the dynamics of the system. The calculations were performed using 4000 points after 2000 transients. The value found was $\lambda \approx 0.01643$ (assuming a sampling frequency of 1Hz).

3 CML identification

It is important to consider first the measurement system for the spatio-temporal system described by the CML model (1). In practice this concerns the number, spatial distribution of the measurement sensors and the form of measurement equation associated with the state-space CML model. Depending on the measurement function the resulting input/output equations may or may not preserve the regularity of the CML model. This aspect has been investigated in Billings and Coca (2000).

A reasonable assumption is that the same measurement devices are used at each spatial location so that the measurement functions are identical at each lattice node. It is also natural to expect that the measurement function will depend only on a finite number of state and input variables in the neighbourhood of the measurement location. For simplicity here the measurement functions are assumed to be

$$\begin{aligned} z_i^x(t) &= x_i(t) \\ z_i^y(t) &= y_i(t) \quad i \in \mathcal{I} \end{aligned} \quad (16)$$

The CML equations can be recovered in this case using only a finite number of measurement locations. The identification of the CML equations (1) requires in fact only the output measurements at the i th lattice site $x_i^{(N)} = \{x_i(1), \dots, x_i(N)\}$, $y_i^{(N)} = \{y_i(1), \dots, y_i(N)\}$ and from neighbouring lattice nodes $s^2 x_i^{(N)} = \{s^2 x_i(1), \dots, s^2 x_i(N)\}$ and $s^2 y_i^{(N)} = \{s^2 y_i(1), \dots, s^2 y_i(N)\}$. In this case the minimum measurement vector required is

$$z = (x_i, s^2 x_i, y_i, s^2 y_i) \quad (17)$$

In practice, if the exact coupling variables are not known in advance, a larger measurement vector which includes coupling variables from a larger neighbourhood can be considered initially. The identification algorithm can then be used to select the true coupling variables.

If the measurements $s^2 x_i^{(N)}$ and $s^2 y_i^{(N)}$ are viewed as inputs, equation (1) is equivalent to a multivariable NARX model [11]

$$z'(t) = f(z'(t-1), \dots, z'(t-n_y), u(t-1), \dots, u(t-n_u)) \quad (18)$$

where $z'(t) = (x_i(t), y_i(t))$ and $u(t) = (s^2 x_i(t), s^2 y_i(t))$. It follows that the lattice equations (1) can be identified using a modified version [2] of the standard nonlinear system identification algorithm [1].

Assuming that the form of the function f is not known, the input output equation can be approximated from the available data using a known set of basis functions or regressors φ_k

$$z'(t) = \sum_{k \in K} \theta_k \varphi_k(z'(t-1), \dots, z'(t-n_y), u(t-1), \dots, u(t-n_u)) + e(t) \quad (19)$$

normally selected from a considerably larger regressor set \mathcal{M} . In equation (19) $\Theta = \{\theta_k\}_{k \in K}$ denotes the parameter vector. Typical regressor classes used in nonlinear system identification include polynomial and rational functions, radial basis functions (RBF) and wavelets. In this particular case the CML equations were approximated using polynomial functions. The selection of the relevant terms in the model (structure selection) and the estimation of the model parameters was performed using the Orthogonal Forward Regression Algorithm which is detailed in [1].

In order to enforce the symmetry of the coupling topology and of the coupling functions during the selection stage, the polynomial regressor set has to be modified accordingly in order to ensure the symmetry of the coupling function f_c in (1). That is, the standard polynomial regressors which include the input variables (which correspond to the coupling variables at site i) are replaced with symmetric combinations of the respective polynomial terms.

The identification was performed using 1000 data points recorded after 2000 transients from the site $i = (10, 10)$ and the four nearest neighbours namely $i - p^1 = (9, 10)$, $i + p^1 = (11, 10)$, $i - p^2 = (10, 9)$, $i + p^2 = (10, 11)$ where as before $p^1 = (1, 0)$ and $p^2 = (0, 1)$. This corresponds to the output vector given in (17). By setting $n_x = n_y = 1$, the model set consisted of all possible polynomial terms corresponding to a fourth-order polynomial with four variables. In this case the coupling variables have been replaced by the aggregated variables

$$\begin{aligned} x_i^*(t-1) &= x_{i_1, i_2-1}(t-1) + x_{i_1, i_2+1}(t-1) + x_{i_1-1, i_2}(t-1) + x_{i_1+1, i_2}(t-1) \\ y_i^*(t-1) &= y_{i_1, i_2-1}(t-1) + y_{i_1, i_2+1}(t-1) + y_{i_1-1, i_2}(t-1) + y_{i_1+1, i_2}(t-1) \end{aligned} \quad (20)$$

The final model identified from the data, which includes only 10 polynomial terms in each equation, is detailed in table (3). Notice that the identification algorithm has determined that only 10 polynomial terms are required in each equation. The algorithm has therefore selected the most significant 10 terms from a total set of 70 possible model terms. The resulting model is structurally different from the original model which included exponential functions. However, the simulation results below show that the original and the identified CML models exhibit very similar dynamics. The algorithm can also deal effectively with noise corrupted observations. The identification of a stochastic equivalent of the CML model (1) has been addressed in a previous study [4].

The estimated model was simulated for 6000 steps using the same set of initial conditions as the original model. To avoid negative populations $x_i(t)$ and $y_i(t)$ are set to zero whenever $x_i(t) < 0$ and $y_i(t) < 0$ respectively.

The identification data superimposed with the estimated model one-step-ahead predictions at that location are plotted in Figure 1. The fact that the predictions for the y variable are less accurate than for the x variable, especially in the lower part of the graph, is due to resetting the value of y to zero whenever it becomes negative. For comparison, snapshots of the x and y lattice after 6000 steps are shown for both the original (Figs. 2a,b) and the identified (Figs. 3a,b) model.

Figures 4a,b show the phase-plots computed using the prey and predator populations at the $i = (10, 10)$ site for the original and the estimated model respectively. In addition, the largest Lyapunov exponent computed from 4000 data points of the global population was found to be $\lambda_{est} \approx 0.0161$, which is in good agreement with the original value of $\lambda \approx 0.01643$

Output	Terms	Estimates	$[ERR]_i$	Std. Dev.
$x_i(t)$	$x_i^*(t-1)^a$	$0.18681E-3$	$0.76254E+0$	$0.16808E-3$
	$x_i(t-1)^2 y_i(t-1)^2$	$-0.20811E+2$	$0.69328E-1$	$0.15646E+0$
	const	$0.48373E-2$	$0.56845E-1$	$0.52838E-3$
	$y_i(t-1)$	$-0.11080E-1$	$0.48190E-1$	$0.36903E-2$
	$x_i(t-1)y_i(t-1)^2$	$0.31777E+2$	$0.16287E-1$	$0.10095E+0$
	$x_i(t-1)$	$0.39354E+1$	$0.12106E-1$	$0.40197E-2$
	$x_i(t-1)^2$	$-0.38672E+1$	$0.23609E-1$	$0.58973E-2$
	$x_i(t-1)y_i(t-1)$	$-0.18105E+2$	$0.76011E-2$	$0.35284E-1$
	$x_i(t-1)^2 y_i(t-1)$	$0.16419E+2$	$0.28314E-2$	$0.59870E-1$
	$x_i(t-1)y_i(t-1)^3$	$-0.18773E+2$	$0.62059E-3$	$0.13397E+0$
$y_i(t)$	$y_i(t-1)$	$0.62376E-2$	$0.81236E+0$	$0.75436E-2$
	$y_i^*(t-1)^b$	$0.19113E+0$	$0.11457E+0$	$0.61833E-3$
	const	$0.50163E-2$	$0.34781E-1$	$0.17464E-2$
	$y_i(t-1)^3$	$-0.99424E+0$	$0.21724E-1$	$0.44305E+0$
	$x_i(t-1)^2 y_i(t-1)^2$	$0.188654E+1$	$0.10787E-1$	$0.33320E+0$
	$y_i(t-1)^2$	$0.69317E+0$	$0.54517E-2$	$0.24352E+0$
	$x_i(t-1)y_i(t-1)$	$0.46409E+1$	$0.23674E-2$	$0.14133E-1$
	$x_i(t-1)y_i(t-1)^3$	$0.85255E+1$	$0.96791E-3$	$0.44567E+0$
	$y_i(t-1)$	$-0.80802E+0$	$0.42886E-3$	$0.38111E-1$
	$x_i(t-1)y_i(t-1)^2$	$-0.11015E+2$	$0.25205E-3$	$0.76680E+0$

^a $x_i^*(t-1) = x_{i_1, i_2-1}(t-1) + x_{i_1, i_2+1}(t-1) + x_{i_1-1, i_2}(t-1) + x_{i_1+1, i_2}(t-1)$
^b $y_i^*(t-1) = y_{i_1, i_2-1}(t-1) + y_{i_1, i_2+1}(t-1) + y_{i_1-1, i_2}(t-1) + y_{i_1+1, i_2}(t-1)$

4 Conclusions

The results in this paper open up a new avenue of investigation in the study of spatio-temporal systems. It has been shown that it is possible to extract the local evolution equation for a spatially extended system using only measurements from a limited number of spatial locations and, assuming the equations are space-invariant, to reconstruct the global dynamics of the system. This is extremely useful where practical limitations preclude access to the full state of the system.

The identification procedure has been illustrated using a CML model of interacting (predator-prey) populations which exhibits chaotic spiral waves. Phase-plots and the largest Lyapunov exponent were used to compare the dynamics of the original and the identified models.

5 Acknowledgment

The authors gratefully acknowledge that this research was supported by the UK Engineering and Physical Sciences Research Council.

Figure Captions

Figure 1: Original (circles) and Estimated Model (crosses) One-Step-Ahead Predictions: (a) $x_{10,10}(t)$ (b) $y_{10,10}(t)$

Figure 2: Original CML Model Predicted Populations: (a) Prey $x_i(t)$ and (b) Predator $y_i(t)$

Figure 3: Estimated CML Model Predicted Populations: (a) Prey $x_i(t)$ and (b) Predator $y_i(t)$

Figure 4: Local Attractors at site (10,10): (a) Original CML Model, (b) Estimated CML Model

References

- [1] S. A. Billings, S. Chen, and M. J. Kronenberg. Identification of MIMO non-linear systems using a forward-regression orthogonal estimator. *Int. J. Control*, 49:2157–2189, 1988.
- [2] S. A. Billings and D. Coca. Identification of coupled map lattice models of deterministic distributed parameter systems. *Submitted for publication*, 2000.
- [3] V. Booth, T. Erneux, and J. P. Laplante. Experimental and numerical study of weakly coupled bistable chemical reactors. *J. Phys. Chem.*, 97, 1995.
- [4] D. Coca and S. A. Billings. Coupled map lattice model identification of stochastic distributed parameter systems. *Submitted for publication*, 2000.
- [5] M. C. Cross and P. C. Hohenberg. Pattern formation out of equilibrium. *Reviews-of-Modern-Physics*, 65(3):851–1112, 1993.
- [6] J. Crutchfield and K. Kaneko. Phenomenology of spatio-temporal chaos. In Hao Bai Lin, editor, *Directions in Chaos*, pages 272–353. World Scientific, Singapore, 1987.
- [7] K Kaneko. Spatiotemporal intermittency in coupled map lattices. *Progress of Theoretical Physics*, 74(5):1033–1044, 1985.
- [8] K Kaneko. Turbulence in coupled map lattices. *Physica D*, 18:475–476, 1986.
- [9] K Kaneko. Pattern dynamics in spatiotemporal chaos. pattern selection, diffusion of defect and pattern competition intermittency. *Physica D*, 34:1–41, 1989.
- [10] K. Kaneko, editor. *Coupled Map Lattices: Theory and Experiment*. World Scientific, Singapore, 1993.
- [11] I. J. Leontaritis and S. A. Billings. Input-output parametric models for non-linear systems- Part I: Deterministic non-linear systems. *Int. J. Control*, 41:303–328, 1985.
- [12] N. Platt and S. Hammel. Pattern formation in driven coupled map lattices. *Physica A*, 239(1-3):296–303, 1997.
- [13] S. Sinha and N. Gupte. Adaptive control of spatially extended systems: Targeting spatiotemporal patterns and chaos. *Physical Review E*, 58(5):5221–5224, 1998.
- [14] R. V. Sole, J. Valls, and Bascompte J. Spiral waves, chaos and multiple attractors in lattice models of interacting populations. *Physics Letters A*, 166(2):123–128, 1992.
- [15] T. Yanagita. Phenomenology of boiling: A coupled map lattice model. *Chaos*, 2(3):343–350, 1992.

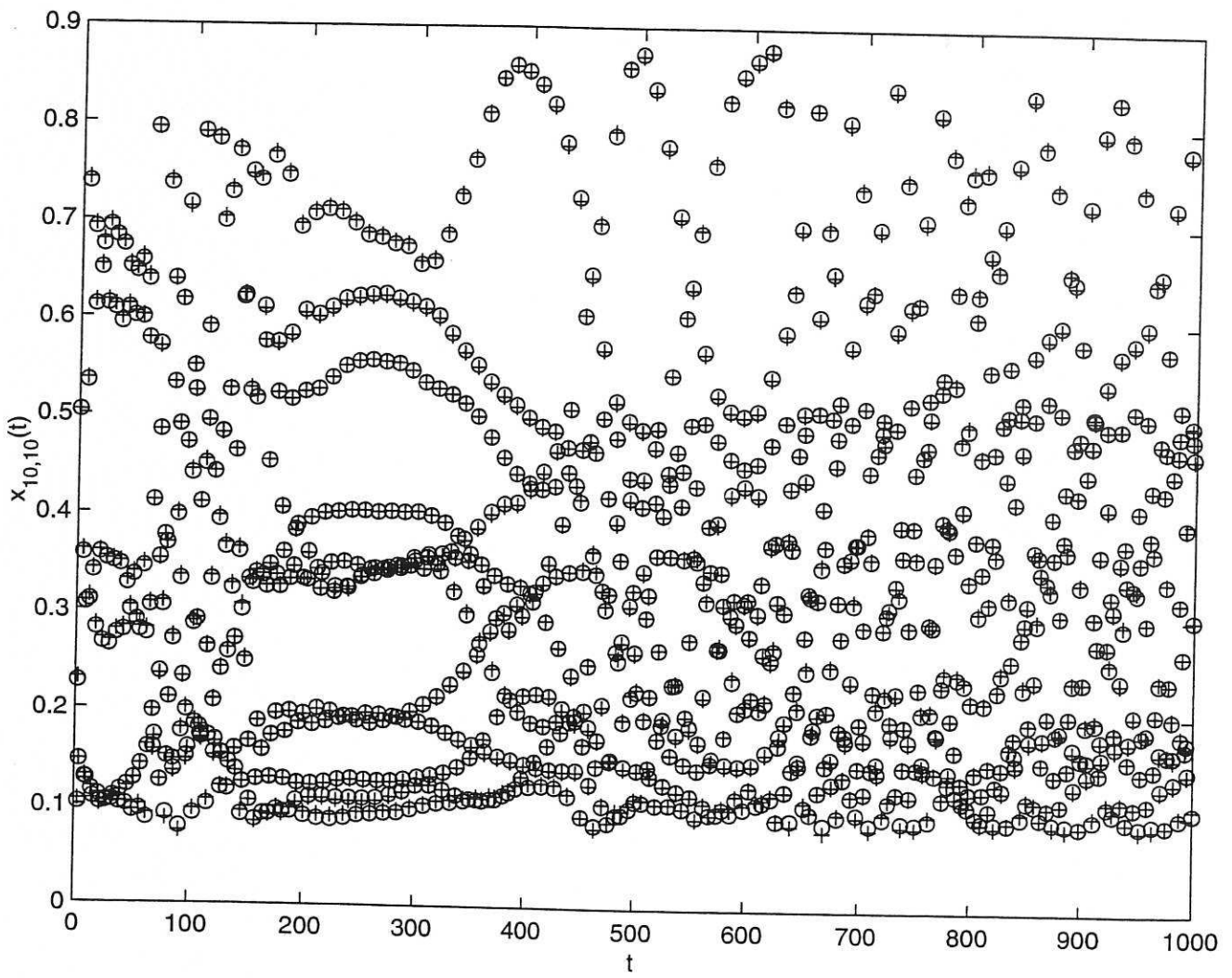


Fig. 1a

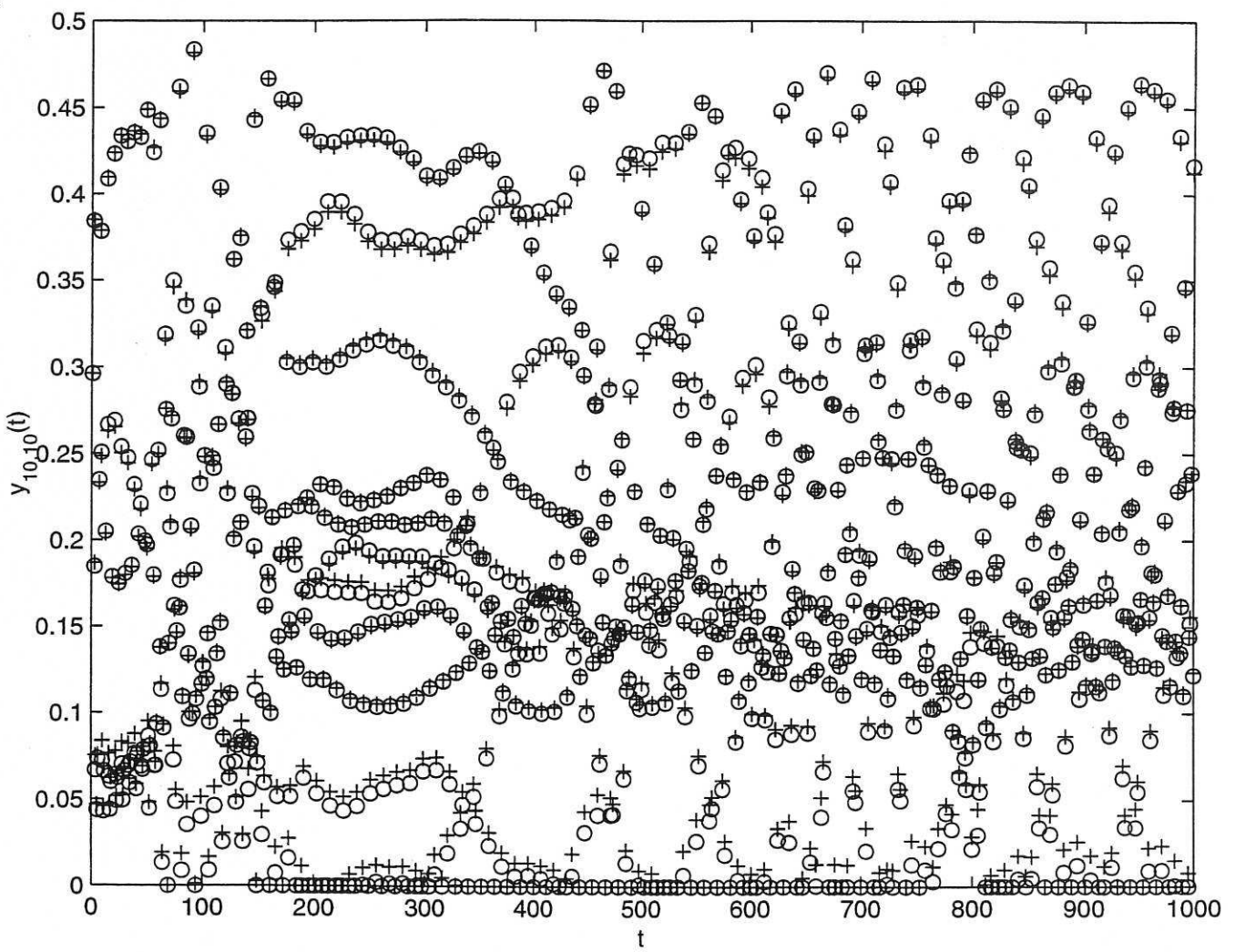


Fig 16.

$x(i,j)$

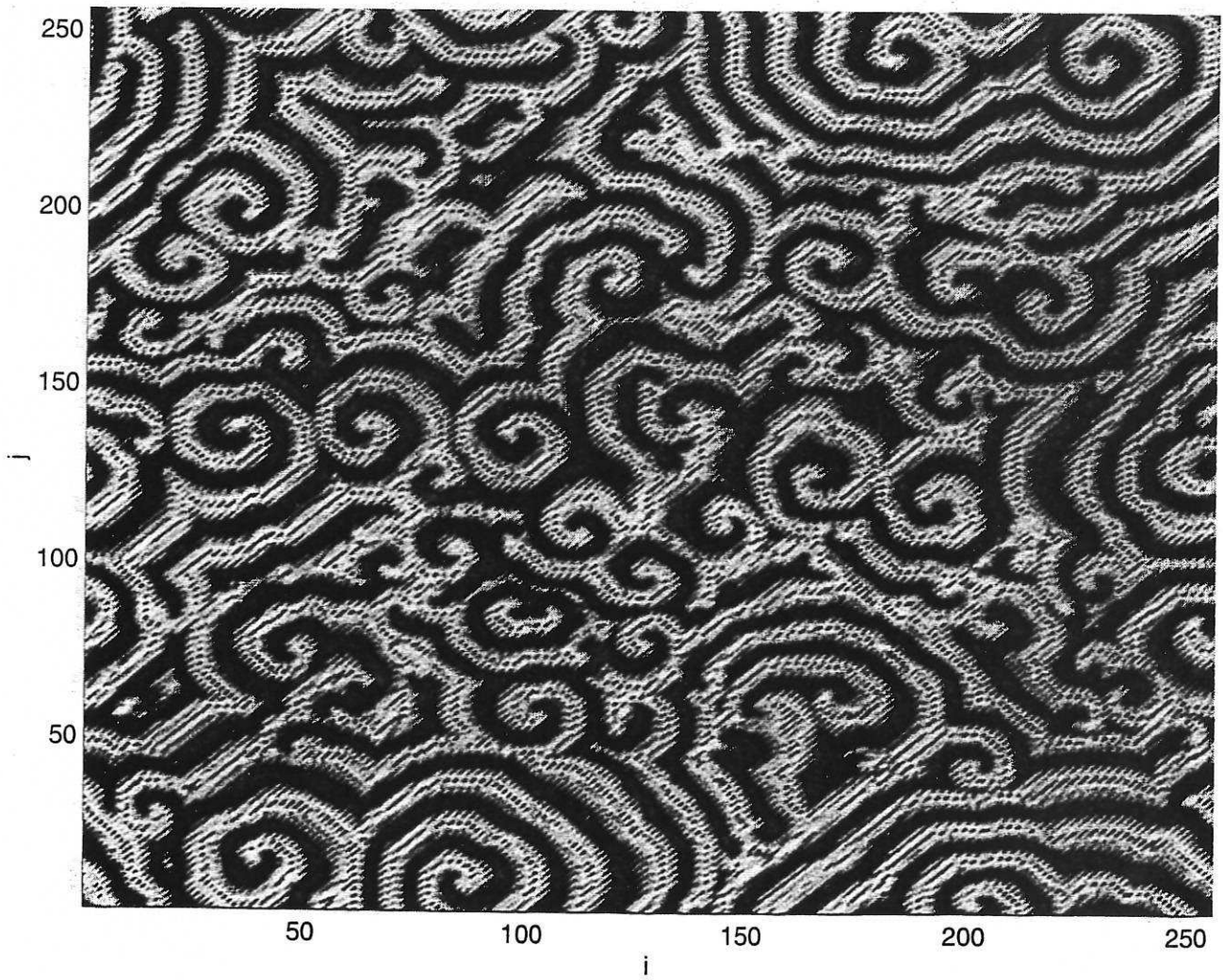


Fig 2a

$y(i,j)$

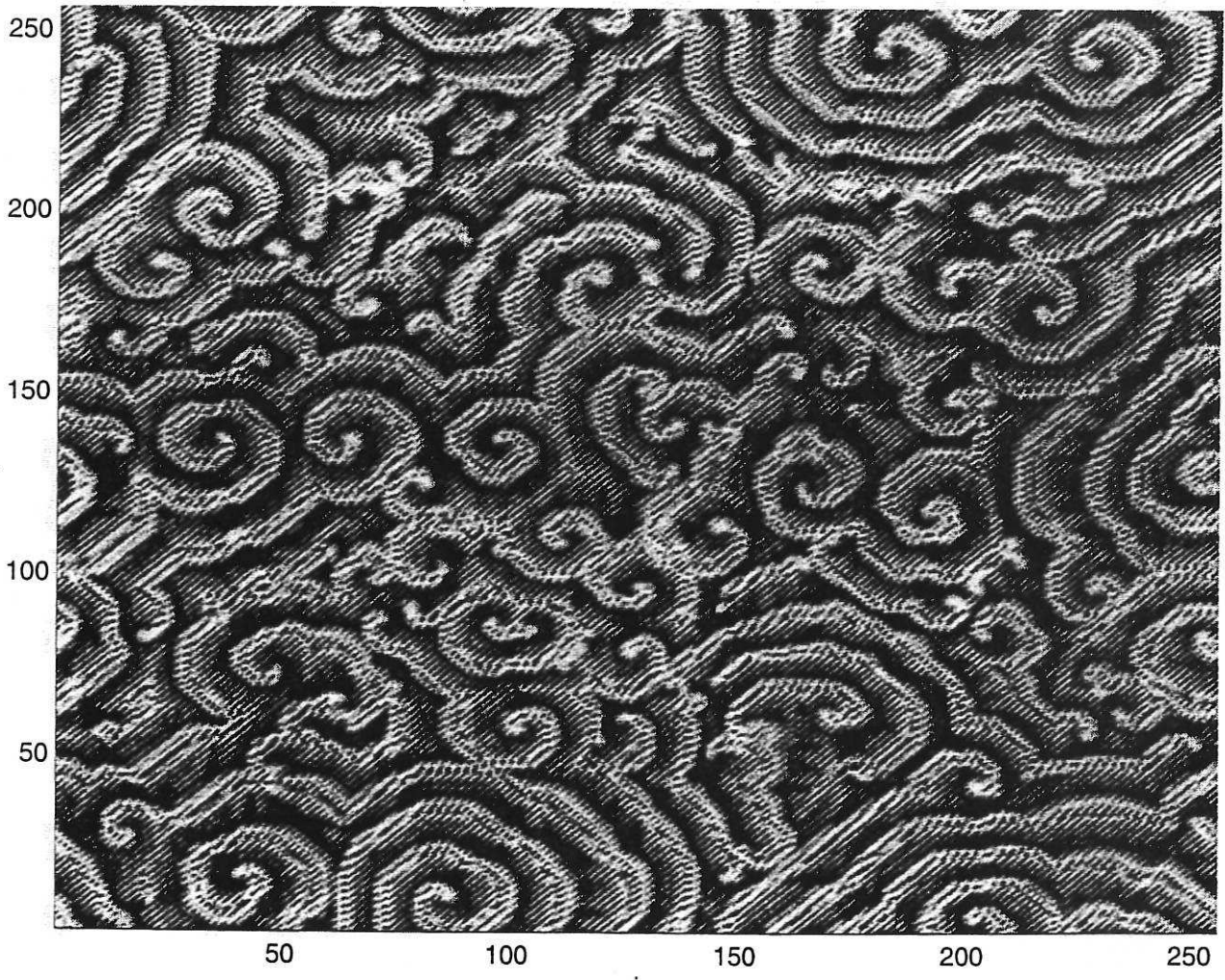


Fig 20

$x(i,j)$

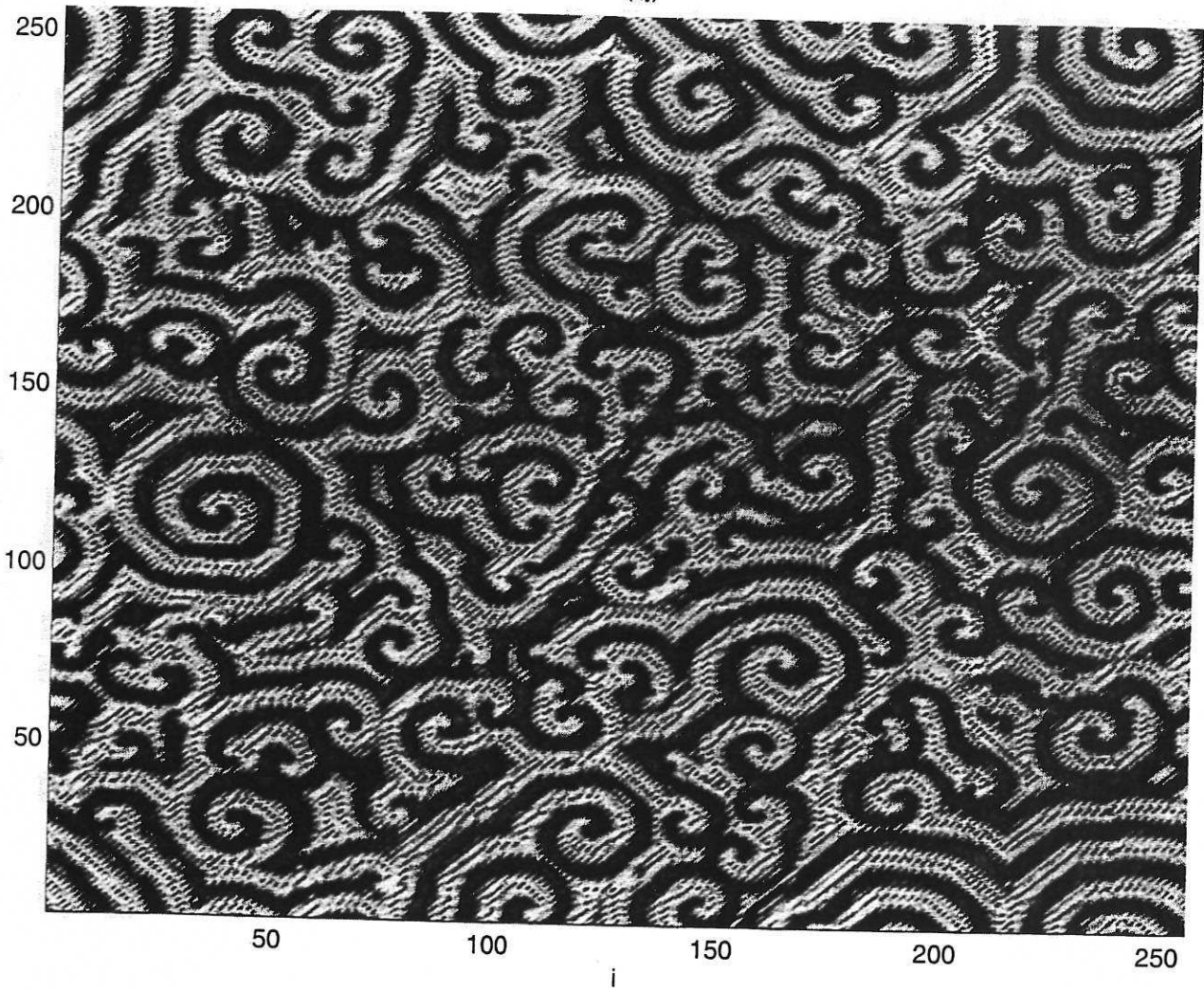


Fig 3a

$y(i,j)$

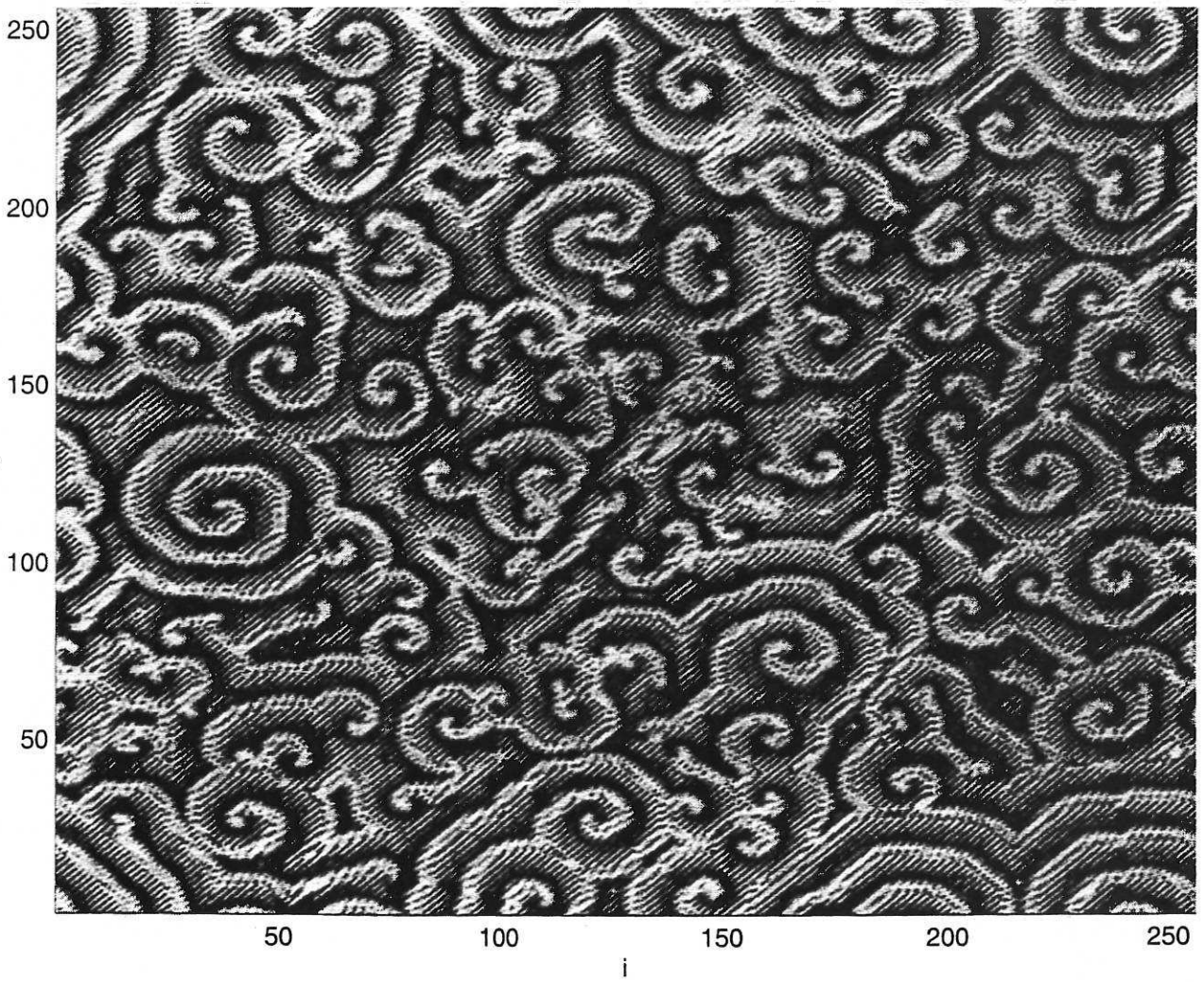


Fig 5.6

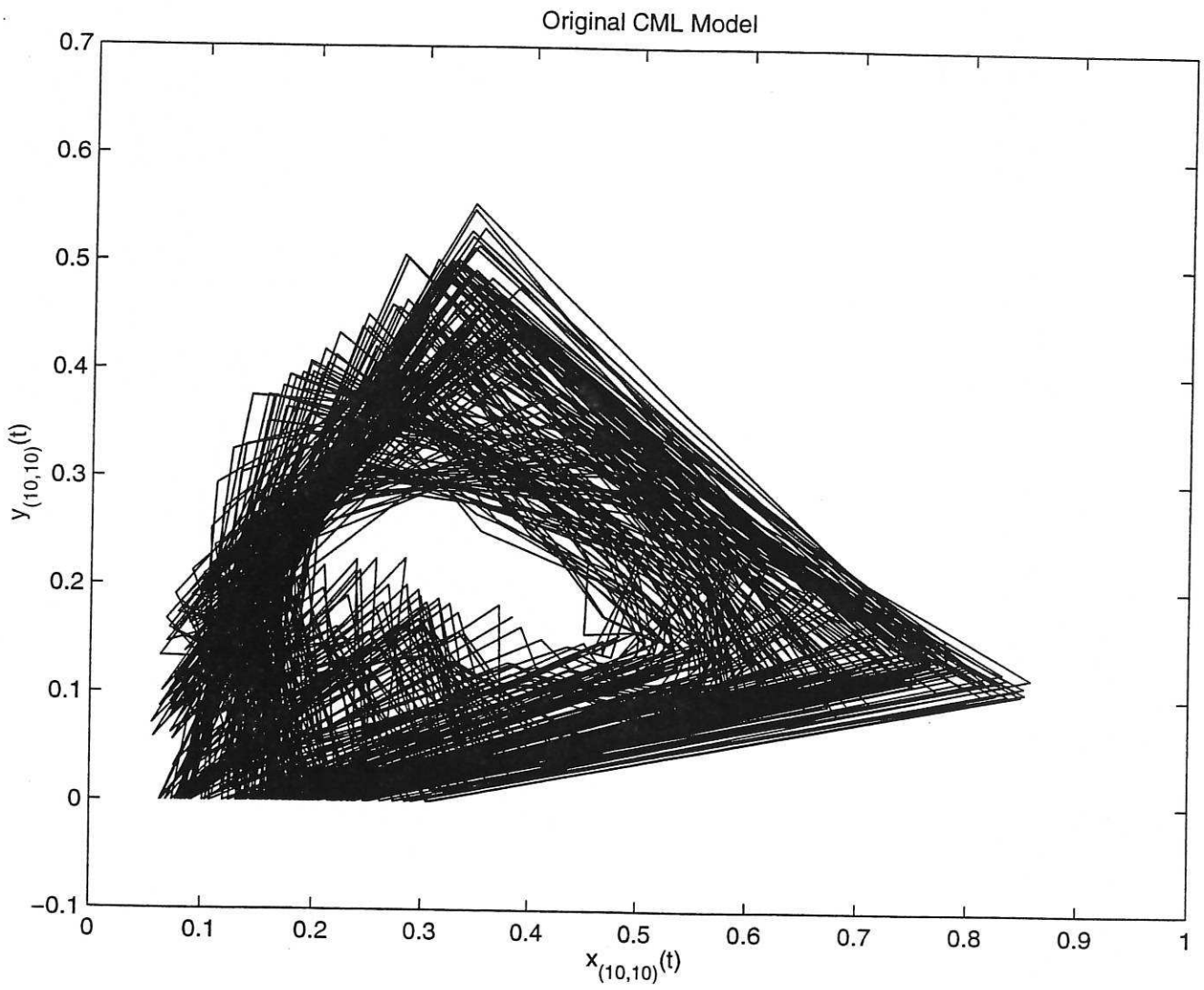


Fig 2a

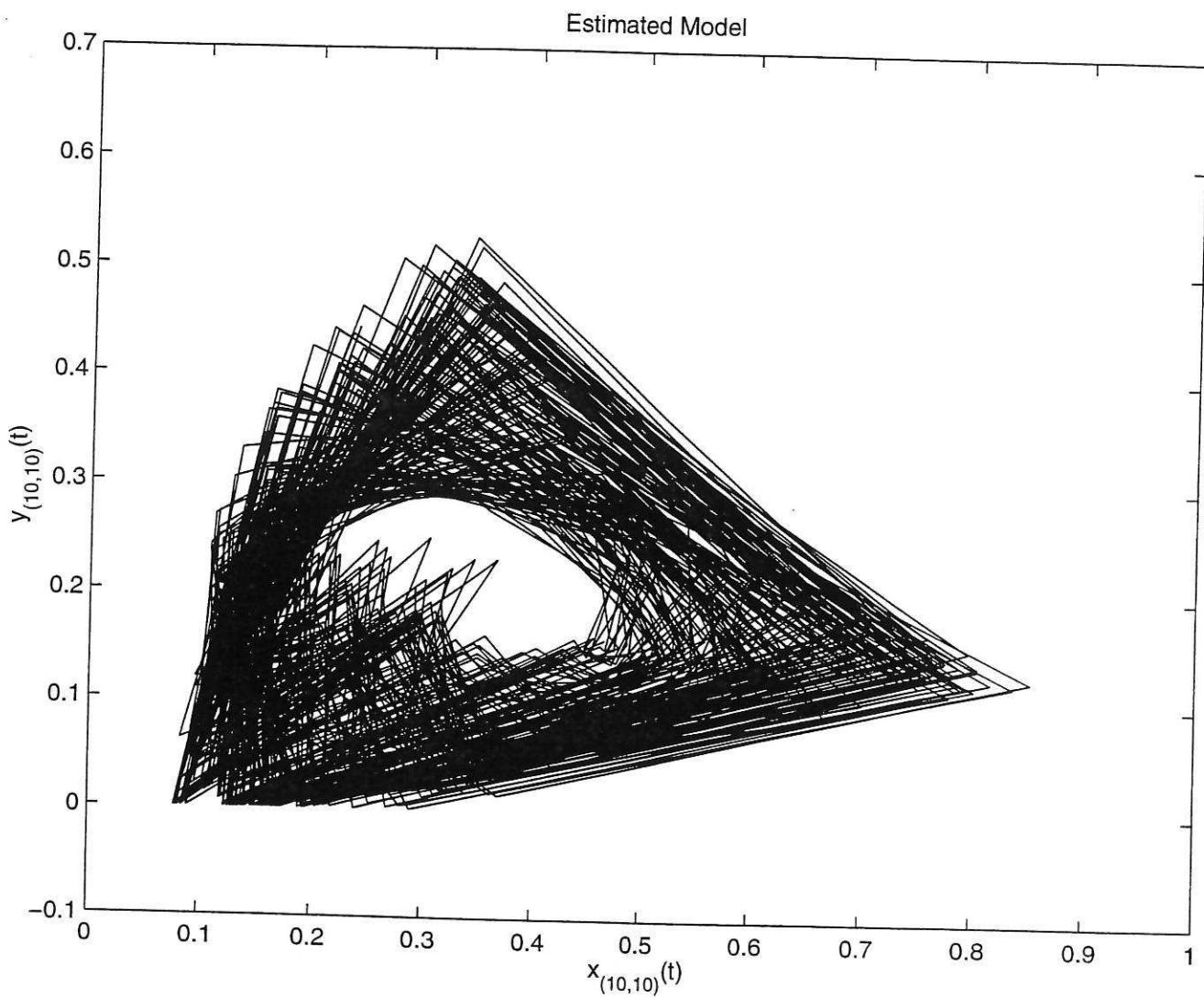


Fig 26

